# Self-degradable imidazolium oligomers as eco-friendly antimicrobials

Yuan Yuan [#,1], Diane S. W. Lim [#,1], Hong Wu [2], Hong Fang Lu [2], Yiran Zheng [1], Andrew Wan [1], Jackie Y. Ying *[,2], Yugen Zhang *[,1]

[1] *Institute of Bioengineering and Nanotechnology, 31 Biopolis Way, Singapore 138669, Singapore*

[2] *NanoBio Lab, 31 Biopolis Way, Singapore 138669, Singapore*

[#] These authors contributed equally to this work.

* Corresponding authors.

*E-mail addresses:* jyying@nbl.a-star.edu.sg (J. Y. Ying), ygzhang@ibn.a-star.edu.sg (Y. G. Zhang).

**Abstract**

Antimicrobial resistance (AMR) has become a global public health threat. One of the major causes of AMR development is the accumulation of low levels of antimicrobials in the environment. To tackle this problem, novel antimicrobial agents that do not leave active residues after treatment are needed. In this study, we present a strategy for synthesizing a series of main-chain imidazolium oligomers that incorporate carbonate, ester, hemiaminal and urea functional groups to serve as degradable linkers. These oligomers exhibit excellent microbicidal activity and kill a broad range of microbes at low concentrations in a short time (99% killing efficiency in 2 min). Moreover, the oligomers are self-degradable and biocompatible. The degradation of these oligomers was studied in buffered solutions with different pH. Under basic conditions (pH = 8), carbonate-linked and ester-linked oligomers degraded to inactive and less toxic small molecules within weeks, making it less likely for these oligomers to induce antimicrobial resistance as compared to traditional antibiotics. The application of these oligomers for *in vivo* treatment of *S. aureus* infected wounds was demonstrated in a mouse model. Notably, the oligomers demonstrated antibacterial efficacy and accelerated wound healing comparable to vancomycin, an antibiotic for first-line treatment of complicated skin infections.

*Keywords:* Main-chain imidazolium oligomer, self-degradable antimicrobials, antimicrobial resistance, broad spectrum antimicrobial agent, haemocompatible, *in vivo* bactericidal activity, *Staphylococcus aureus* infected wound.

## 1. Introduction

Antimicrobial resistance (AMR) is one of the most critical healthcare challenges facing modern society, and is predicted to cause an additional 10 million deaths each year by 2050 [1]. The cost of treating antibiotic-resistant infections has been pegged between US$150 million and $30 billion annually as a result of longer hospital stays and higher morbidity [2]. Most troubling of all are the emerging reports of bacterial infections by strains resistant to all existing drugs, which underscore the pressing need to tackle the issue of antibiotic resistance in bacteria [3]. One of the major causes of AMR development is the overuse of antibiotics, including topical and non-therapeutic applications. This results in sub-therapeutic levels of antibiotics accumulating over time, creating the conditions that select antibiotic-resistant bacteria populations. Cross-species and environmental transmission have also led to human AMR-associated diseases in instances whereby antibiotic-resistant bacteria spread in animals and the environment. There is a pressing need for new antimicrobial technologies that can circumvent or reduce the selection pressure for resistant microbial strains and leave no additional burden.

*Staphylococcus aureus* is one of the most common causes of skin and soft-tissue infection. It is responsible for severe infections in the hospital and the community. In addition to its virulence, *S. aureus* has a proclivity for acquiring resistance to a wide range of antibiotics. The glycopeptide antibiotic vancomycin, which has been in clinical use for about 50 years, was the only drug that could be consistently relied upon to treat severe staphylococcal infections, such as methicillin-resistant *S. aureus* (MRSA) [4]. However, the increasing use of vancomycin has led to the appearance of vancomycin and methicillin-resistant *S. aureus*, [5, 6] necessitating an alternative approach to combat MRSA that would ideally circumvent the development of antibiotic resistance.

Over the last decades, antimicrobial peptides (AMPs) have been widely investigated as a novel class of antibiotics. Unlike traditional antibiotics, which target specific cellular activities (e.g., synthesis of DNA, protein, or cell wall), AMPs target the acidic phospholipids, lipopolysaccharides (Gram-negative bacteria) and peptidoglycan layer (Gram-positive bacteria) of cell membranes [7], which are ubiquitous in microorganisms. The cationic/hydrophilic amino acids first interact with negatively charged bacterial membranes

through electrostatic interaction, and then the hydrophobic regions within the AMPs integrate with the bacterial cell membrane resulting in cell lysis and death. Having a high level of cholesterol and low anionic charge places eukaryotic cells out of the target range of many AMPs [8]. Due to this mode of action, AMPs do not easily induce resistance compared to conventional antibiotics [9] (although they may eventually evoke resistance [10,11]), making them powerful weapons in the campaign against antibiotic-resistant bacterial strains. However, commercialization of AMPs as antibiotics for clinical use is hampered by their potential toxicity when injected into the bloodstream, susceptibility to protease degradation, and high manufacturing costs [12,13].

To overcome these problems, a number of synthetic cationic polymers containing ammonium [14,15], phosphonium [16], pyridinium [17,18], or imidazolium [19-21] units that mimic the amphiphilic structure of AMPs have been developed [22-26]. These compounds possess similar properties to AMPs, such as high antimicrobial activity and selectivity for bacterial cells over mammalian cells. They can be conveniently synthesized, and their structures can be easily tuned for specific properties. We have previously developed a series of main-chain imidazolium polymers and oligomers [20,21,27,28]. These poly-imidazolium materials demonstrated high efficacy, biocompatibility and fast killing kinetics against a broad range of bacteria and fungi. Specifically, short linear imidazolium oligomers were demonstrated to be very effective in the treatment of bacterial infection and fungal keratitis in mice.

In this paper, we report on a new series of imidazolium oligomers with degradable linkers incorporated in their structures. The new imidazolium materials retain the excellent antimicrobial properties of the previously reported materials against a broad range of microbes. In addition, they would self-destruct after treatment, leaving no active residue with the potential for secondary contamination and drug resistance development. Using *S. aureus* as a model pathogenic microbe, we demonstrate that these oligomers induce development of resistance at a much slower rate than vancomycin, and are as effective as vancomycin as a treatment for infected skin wounds in a mouse model.

## 2. Materials and methods

### *2.1. General information*

All anhydrous solvents were purchased from Sigma-Aldrich, and used without further purification. All other reagents were used as received, except where otherwise noted in the experimental text. Microbial broths were prepared using Muller Hinton Broth (MHB) powder

(BD Diagnostics). *S. aureus* (ATCC No. 6538), *E. coli* (ATCC No. 8739), *P. aeruginosa* (ATCC No. 15442) and *C. albicans* (ATCC No. 10231) were obtained from ATCC, U.S.A.

Analytical thin layer chromatography (TLC) was performed using Merck 60 F-254 silica gel plates with visualization by ultraviolet light (254 nm) and/or heating the plate after staining with a solution of 20% $KMnO_4$ w/v in $H_2O$. Flash column chromatography was conducted on Kieselgel 60 (0.040–0.063 mm) supplied by Merck under positive pressure.

$^1H$ and $^{13}C$ nuclear magnetic resonance (NMR) spectra were recorded on Bruker AV-400 (400 MHz) spectrometer. Chemical shifts (δ) were reported in parts per million (ppm) with the residual solvent peak of tetramethylsilane used as the internal standard at 0.00 ppm. $^1H$ NMR data were reported in the following order: chemical shift, multiplicity (br = broad, s = singlet, d = doublet, t = triplet, q = quartet and m = multiplet), coupling constants (*J*, Hz), integration and assignment. High-resolution mass spectra (HRMS) were recorded on a Bruker MicroTOF-Q system. The samples were directly injected into the chamber at 20 $\mu L \cdot min^{-1}$. Typical instrument parameters were capillary voltage: 4 kV, nebulizer: 0.4 bars; dry gas: 2 $L \cdot min^{-1}$ at 120 °C, and *m/z* range: 40–3000.

*2.2. Synthesis of degradable linkers*

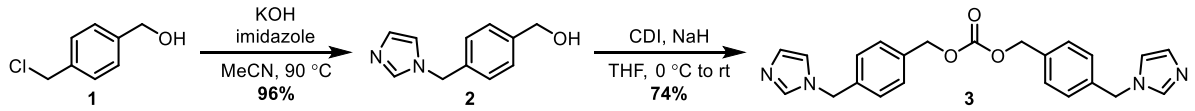


**[4-(1H-Imidazol-1-yl)methylphenyl]methanol (2).** A two-neck round-bottom flask fitted with a dropping funnel and reflux condenser was filled with imidazole (871 mg, 12.8 mmol) and powder KOH (1.16 g, 16.6 mmol). Acetonitrile (70 mL) was added to the flask, and the mixture was stirred at 25 °C over 1 h. The dropping funnel was then charged with a solution of benzyl chloride **1** (2.00 g, 12.8 mmol) in acetonitrile (57 mL) that was added dropwise to the stirring mixture. Upon complete addition, the reaction mixture was stirred at reflux over 16 h, then cooled to room temperature and concentrated under reduced pressure. The resultant solids were dissolved in chloroform (20 mL) and washed with water (20 mL). The aqueous layer was then extracted with ethyl acetate (2 × 20 mL). The combined organic layers were dried over $Na_2SO_4$, filtered and concentrated under reduced pressure to obtain benzyl alcohol **2** as a yellow oil (2.31 g, 12.3 mmol, 96%). **$^1$H NMR** (400 MHz, $CDCl_3$) δ 7.42 (s, 1H, ImH), 7.33 (d, *J* = 8.0 Hz, 2H, PhH), 7.08 (d, *J* = 8.0 Hz, 2H, PhH), 6.97 (t, *J* = 1.0 Hz, 1H, ImH), 6.85 (d, *J* = 1.0 Hz, 1H, ImH), 5.04 (s, 2H, $NCH_2$), 4.66 (s, 2H, $OCH_2$). **$^{13}$C NMR** (101 MHz, $CDCl_3$) δ 141.4, 137.4, 135.3, 129.7, 127.5, 119.3, 64.6, 50.6.

**Bis[4-(1H-Imidazol-1-yl)methylbenzyl] carbonate (3).** 1,1'-carbonyldiimidazole (CDI, 1,03 g, 6.35 mmol) was added to a solution of benzyl alcohol **2** (1.20 g, 6.35 mmol) in anhydrous THF (20 mL) at 0 °C in one portion. The solution was stirred and warmed to room temperature over 2 h. In the meantime, a second solution of benzyl alcohol **2** (1.20 g, 6.35 mmol) in anhydrous THF (20 mL) was cooled to 0 °C. NaH (60% dispersion in mineral oil, 254 mg, 6.35 mmol) was added to the second solution, and the mixture was stirred at 0 °C for 30 min. The solution of benzyl carbamate was then added slowly to the solution of deprotonated benzyl alcohol at 0 °C, and the resulting mixture was warmed to room temperature over 1 h. The reaction mixture was diluted with ethyl acetate (10 mL), and quenched with saturated aqueous $NH_4Cl$ (50 mL). The aqueous layer was extracted with ethyl acetate (2 × 30 mL), and the combined organic layers were dried over $Na_2SO_4$, filtered and concentrated under reduced pressure. The resulting crude material was purified by column chromatography (1% MeOH in $CHCl_3$) to obtain carbonate **3** as an off-white solid (1.90 g, 4.72 mmol, 74%). **$^1$H NMR** (400 MHz, $CDCl_3$) δ 7.54 (s, 2H, ImH), 7.36 (d, *J* = 8.0 Hz, 4H, PhH), 7.14 (d, *J* = 8.0 Hz, 4H, PhH), 7.09 (s, 2H, ImH), 6.89 (s, 2H, ImH), 5.15 (s, 4H, $OCH_2$), 5.12 (s, 4H, $NCH_2$). **$^{13}$C NMR** (101 MHz, $CDCl_3$) δ 154.9, 137.4, 136.6, 135.2, 129.9, 128.9, 127.5, 119.3, 69.2, 50.4.

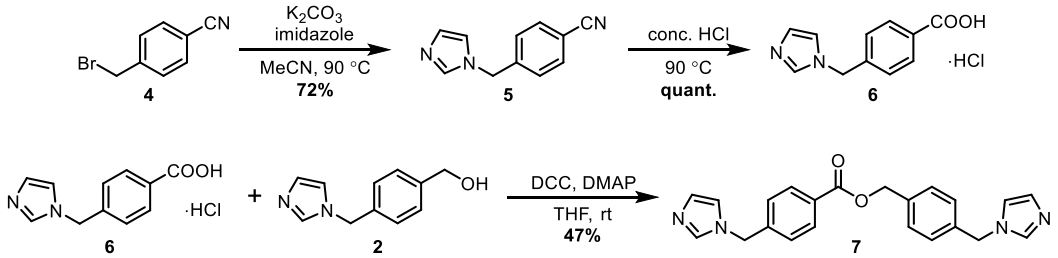


**4-[(1H-Imidazol-1-yl)methyl]benzonitrile (5).** To a solution of benzyl bromide **4** (3.00 g, 15.3 mmol) in acetonitrile (50 mL) in a two-neck round-bottom flask fitted with a reflux condenser was added imidazole (3.10 g, 45.9 mmol), followed by solid $K_2CO_3$ (10.6 g, 76.5 mmol). The reaction mixture was stirred under reflux over 16 h, and then cooled to room temperature and filtered through cotton wool. The filtrate was concentrated, and the resultant solids were re-dissolved in dichloromethane (50 mL). The organic solution was washed with saturated aqueous sodium carbonate solution (2 × 30 mL), dried over $Na_2SO_4$, filtered and concentrated under reduced pressure to obtain benzonitrile **5** as a yellow powder (2.01 g, 11.0 mmol, 72%). **$^1$H NMR** (400 MHz, $CDCl_3$) δ 7.66 (d, *J* = 8.5 Hz, 2H, PhH), 7.57 (s, 1H, ImH), 7.22 (d, *J* = 8.5 Hz, 2H, PhH), 7.14 (s, 1H, ImH), 6.91 (s, 1H, ImH), 5.21 (s, 2H,

$NCH_2$). **$^{13}$C NMR** (101 MHz, $CDCl_3$) δ 141.6, 137.6, 132.9, 130.5, 127.6, 119.3, 118.3, 112.4, 50.2.

**4-[(1H-Imidazol-1-yl)methyl]benzoic acid (6).** Benzonitrile **5** (100 mg, 0.546 mmol) was dissolved in 37% concentrated hydrochloric acid (1.5 mL) and stirred at reflux for 3 h. The solution was cooled to room temperature, then concentrated under reduced pressure to obtain carboxylic acid **6** as a white solid (130 mg, 0.546 mmol, quant.). **$^1$H NMR** (400 MHz, $d_4$-MeOD) δ 7.86 (d, *J* = 8.5 Hz, 2H, PhH), 7.78 (s, 1H, ImH), 7.32 (d, *J* = 8.5 Hz, 2H, PhH), 7.14 (s, 1H, ImH), 7.01 (s, 1H, ImH), 5.31 (s, 2H, $NCH_2$); **$^{13}$C NMR** (101 MHz, $d_4$-MeOD) δ 171.8, 142.3, 138.8, 134.7, 129.5, 129.3, 128.5, 121.0, 51.1.

**4-[(1H-Imidazol-1-yl)methyl]benzyl 4-[(1H-imidazol-1-yl)methyl]benzoate (7).** To a solution of carboxylic acid **6** (193 mg, 0.808 mmol) and DMAP (85 mg, 0.699 mmol) in anhydrous THF (35 mL) was added a solution of benzyl alcohol **2** (101 mg, 0.538 mmol) and DCC (111 mg, 0.538 mmol) in anhydrous THF (35 mL). The resulting mixture was stirred at room temperature over 12 h, and filtered through cotton wool. The filtrate was concentrated and the resulting solids were dissolved in ethyl acetate (10 mL) and washed with saturated aqueous $NaHCO_3$ (2 × 10 mL). The organic layer was dried over $Na_2SO_4$, filtered and concentrated under reduced pressure. The resulting crude material was purified by column chromatography (0 → 5% MeOH in $CHCl_3$) to obtain ester **7** as a white solid (94 mg, 0.252 mmol, 47%). **$^1$H NMR** (400 MHz, $CDCl_3$) δ 8.04 (d, *J* = 8.0 Hz, 2H, PhH), 7.55 (s, 1H, ImH), 7.54 (s, 1H, ImH), 7.42 (d, *J* = 8.0 Hz, 2H, PhH), 7.20–7.16 (m, 4H, PhH), 7.10 (s, 1H, ImH), 7.08 (s, 1H, ImH), 6.89 (s, 2H, ImH), 5.34 (s, 2H, $OCH_2$), 5.18 (s, 2H, $NCH_2$), 5.12 (s, 2H, $NCH_2$). **$^{13}$C NMR** (101 MHz, $CDCl_3$) δ 165.7, 141.5, 137.5, 137.4, 136.3, 136.0, 130.4, 130.0, 129.9, 129.8, 128.8, 127.5, 127.1, 119.3, 66.3, 50.4, 50.3.

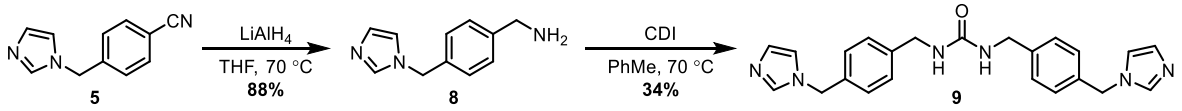

5 8 9

**4-(1H-Imidazol-1-yl)methylphenylmethanamine (8).** To a three-neck round-bottom flask fitted with a dropping funnel and reflux condenser was added solid $LiAlH_4$ (1.70 g, 43.9 mmol), followed by anhydrous THF (12 mL). The suspension was heated at a gentle reflux. The dropping funnel was then charged with a solution of benzonitrile **5** (2.01 g, 11.0 mmol) in anhydrous THF (35 mL), which was added dropwise to the refluxing mixture over the course of 1 h. The resulting thick brown slurry was stirred at reflux over 16 h, then cooled to 0 °C and quenched carefully with water (10 mL) until it formed a thick white slurry. The pH

of the slurry was adjusted to 12 with 3 M aqueous NaOH, and the resulting mixture was filtered through Celite® that was rinsed with dichloromethane. The organic layer from the filtrate was collected, and the aqueous layer was extracted with dichloromethane (2 × 20 mL). The combined organic layers were dried over $Na_2SO_4$, filtered and concentrated under reduced pressure to obtain benzylamine **8** as a yellow oil (1.81 g, 9.67 mmol, 88%). **$^1$H NMR** (400 MHz, $CDCl_3$) δ 7.54 (s, 1H, ImH), 7.31 (d, *J* = 8.0 Hz, 2H, PhH), 7.13 (d, *J* = 8.0 Hz, 2H, PhH), 7.08 (s, 1H, ImH), 6.90 (s, 1H, ImH), 5.11 (s, 2H, $NCH_2$), 3.87 (s, 2H, $CH_2NH_2$). **$^{13}$C NMR** (101 MHz, $CDCl_3$) δ 143.4, 137.4, 134.6, 129.8, 127.7, 127.6, 119.2, 50.6, 46.0.

**1,3-Bis[4-(1H-imidazol-1-yl)methylbenzyl]urea (9).** A solution of benzyl amine **8** (1.80 g, 9.82 mmol) and 1,1-carbonyldiimidazole (CDI, 1.17 g, 5.93 mmol) in anhydrous toluene (21 mL) was stirred at 70 °C over 16 h. The resulting mixture was cooled to room temperature and concentrated. The solids obtained were dissolved in dichloromethane (50 mL) and washed with saturated aqueous $Na_2CO_3$ (20 mL). The aqueous layer was extracted with DCM (2 × 10 mL), and the combined organic layers were dried over $Na_2SO_4$, filtered and concentrated under reduced pressure. The resulting crude material was purified by column chromatography (6 → 10% MeOH in dichloromethane) to obtain urea **9** as a white solid (662 mg, 1.65 mmol, 34%). **$^1$H NMR** (400 MHz, $CDCl_3$) δ 7.42 (s, 2H, ImH), 7.17 (d, *J* = 8.0 Hz, 4H, PhH), 7.00 (d, *J* = 8.0 Hz, 4H, PhH), 6.98 (s, 2H, ImH), 6.84 (s, 2H, ImH), 6.01 (t, *J* = 5.5 Hz, 2H, NH), 5.01 (s, 4H, $NCH_2$), 4.27 (d, *J* = 5.5 Hz, 4H, $CH_2NH$). **$^{13}$C NMR** (101 MHz, $CDCl_3$) δ 158.7, 140.1, 137.2, 134.8, 129.4, 127.8, 127.5, 119.4, 50.5, 43.6.

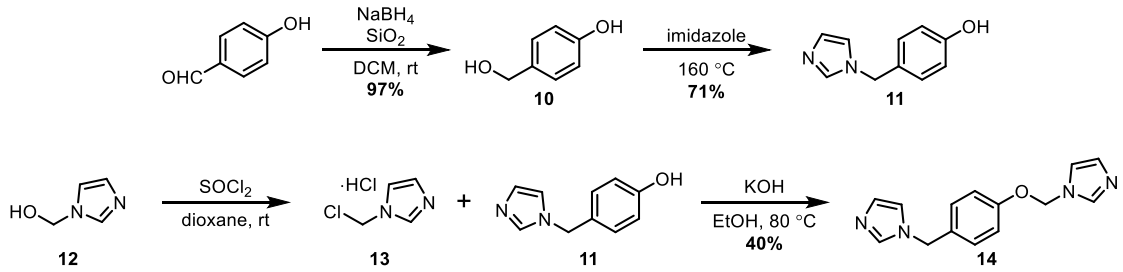


**4-(1H-Imidazol-1-yl)methylphenol (11).** Benzyl alcohol **10** [29] (1.92 g, 15.5 mmol) and imidazole (3.17 g, 46.5 mmol) were combined in vial vented by a needle and heated at 160 °C over 30 min. The hot mixture was poured into boiling water (100 mL), and the hot suspension was filtered through a Büchner funnel. The residue was rinsed with hot water (2 × 10 mL) and dried *in vacuo* (50 °C, 10 mbar) to obtain phenol **11** as a white powder (1.92 g, 11.0 mmol, 71%). **$^1$H NMR** (400 MHz, $d_6$-DMSO) δ 9.50 (br s, 1H, OH), 7.69 (s, 1H, ImH), 7.13 (t, *J* = 1.0 Hz, 1H, ImH), 7.10 (d, *J* = 8.5 Hz, 2H, PhH), 6.87 (t, *J* = 1.0 Hz, 1H, ImH),

6.72 (d, $J$ = 8.5 Hz, 2H, PhH), 5.03 (s, 2H, $NCH_2$). **$^{13}$C NMR** (101 MHz, $d_6$-DMSO) δ 157.0, 137.1, 129.1, 128.6, 128.0, 119.3, 115.3, 49.1.

The spectroscopic data were found to be in agreement with that reported by McNulty and co-workers [29].

**1-(Chloromethyl)-1H-imidazole (13).** To a solution of 1H-imidazole-1-methanol **12** [30] (80% w/w, 1.00 g, 8.15 mmol) in anhydrous dioxane (16 mL) was added $SOCl_2$ (1.8 mL, 24.5 mmol). The reaction mixture was stirred at room temperature over 2 h, then concentrated under reduced pressure to obtain chloride **13** as an off-white syrup (1.79 g). Analysis of the material by $^1$H NMR spectroscopy ($d_6$-DMSO) revealed chloride **13** present as its HCl salt along with imidazole hydrochloride in a 3:2 ratio (69% w/w).

**1-[4-(1H-Imidazol-1-yl)methoxybenzyl]-1H-imidazole (14).** To a solution of chloride **13** (69% w/w, 1.35 g, 6.09 mmol) in EtOH (12 mL) were added phenol **11** (1.06 g, 6.09 mmol) and KOH pellets (1.03 g, 18.3 mmol). The solution was stirred under reflux for 16 h, cooled to room temperature, and filtered through cotton wool. The filtrate was concentrated and the resulting solids were re-dissolved in dichloromethane (10 mL). The organic solution was washed with water (10 mL), followed by 1 M aqueous NaOH (3 × 10 mL), dried over $Na_2SO_4$, filtered and concentrated under reduced pressure to obtain hemiaminal **14** as a yellow oil (616 mg, 2.42 mmol, 40%). **$^1$H NMR** (400 MHz, $d_6$-DMSO) δ 7.87 (s, 1H, ImH), 7.73 (s, 1H, ImH), 7.34 (t, $J$ = 1.5 Hz, 1H, ImH), 7.23 (d, $J$ = 8.5 Hz, 2H, PhH), 7.16 (t, $J$ = 1.5 Hz, 1H, ImH), 7.04 (d, $J$ = 8.5 Hz, 2H, PhH), 6.92 (t, $J$ = 1.0 Hz, 1H, ImH), 6.88 (t, $J$ = 1.0 Hz, 1H, ImH), 5.98 (s, 2H, $OCH_2$), 5.11 (s, 2H, $NCH_2$). **$^{13}$C NMR** (101 MHz, $d_6$-DMSO) δ 155.4, 138.3, 137.3, 131.6, 129.2, 129.0, 128.7, 119.9, 119.5, 116.1, 72.9, 48.9.

*2.3. Synthesis of imidazolium oligomers*

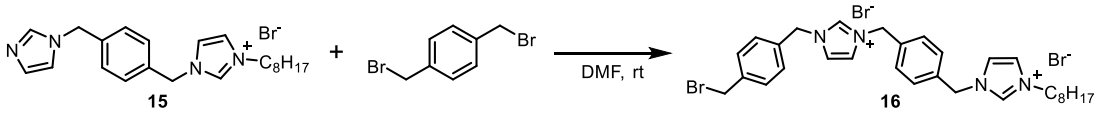


A solution of **15** [27] (2.63 g, 6.23 mmol) in DMF (62 mL) was added dropwise to a solution of 1,4-dibromo-*p*-xylylene (16.4 g, 62.3 mmol) and the resulting mixture was stirred at 25 °C over 48 h. The reaction mixture was concentrated *in vacuo*, and the product was precipitated with ether. The solids were spun down in a Falcon® tube in a centrifuge (5000 rpm), and the supernatant was decanted. The solids were washed with ether followed by acetone. The resulting solids were dried in a vacuum oven (50 °C, 10 mbar) over 16 h to obtain bisimidazolium salt **16** as white solids (2.88 g, 4.44 mmol, 71%). **$^1$H NMR** (400 MHz,

$d_6$-DMSO) δ 9.49 (s, 1H, ImH), 9.39 (s, 1H, ImH), 7.86–7.82 (m, 4H, ImH),7.51–7.40 (m, 8H, PhH), 5.45 (s, 6H, 3 x $NCH_2$), 4.71 (s, 2H, $CH_2Br$), 4.17 (t, J = 7.4 Hz, 2H, $CH_2N$), 1.80–1.76 (m, 2H, $NCH_2CH_2$), 1.31–1.15 (m, 10H, $C_5H_{10}$), 0.85 (t, *J* = 6.5 Hz, 6H, 2 x $CH_3$). **$^{13}$C NMR** (101 MHz, $d_6$-DMSO) δ 138.7, 136.4, 136.2, 135.5, 135.3, 134.9, 129.9, 129.1, 128.9, 128.7, 123.0, 122.9, 122.6, 51.6, 51.5, 51.4, 49.0, 31.2, 29.3, 28.5, 28.3, 25.5, 22.1, 14.0. Unreacted $\alpha,\alpha$'-dibromo-*p*-xylene (~ 8 equiv.) was recovered by concentrating the combined ether washings.

**General procedure for the synthesis of imidazolium oligomers.** Linker (1.0 eq) and bisimidazolium salt (2.4 eq) were dissolved in anhydrous DMF (0.02 M), and stirred at room temperature over 24–48 h. The reaction mixture was concentrated *in vacuo* to ~ 5–10 mL, and the product was precipitated with acetone. The solids were spun down in a Falcon® tube in a centrifuge (5000 rpm), and the supernatant was decanted. They were washed twice more by first dissolving in a minimum amount of methanol, and then precipitated with acetone (total volume of 40–50 mL). The resulting solids were dried in a vacuum oven (50 °C, 10 mbar) over 16 h to obtain the imidazolium oligomers as white powders.

Where DMF was detected in NMR spectroscopic analysis of the compounds, it could be azeotropically removed with toluene. This was achieved by first dissolving the powder in a minimum amount of methanol, adding 3–4 times the volume of toluene, and removing the solvents *in vacuo*. Repeating this step twice was usually sufficient to remove traces of DMF from the samples for biological testing.

**IBN-Carbonate-C8** (**IBN-CC8**) was prepared by the general procedure from carbonate linker **3** and isolated as a white powder (438 mg, 0.244 mmol, 47%). **$^{1}$H NMR** (400 MHz, $d_6$-DMSO) δ 9.56–9.54 (m, 4H, ImH), 9.42 (s, 2H, ImH), 7.86–7.84 (m, 12H, ImH), 7.51–7.43 (m, 24H, PhH), 5.47 (s, 20H, 10 × $NCH_2$), 5.16 (s, 4H, 2 × $OCH_2$), 4.17 (t, *J* = 7.0 Hz, 4H, 2 × $NCH_2CH_2$), 1.80–1.77 (m, 4H, 2 × $NCH_2CH_2$), 1.24–1.23 (m, 20H, 2 × $C_5H_{10}$), 0.85 (t, *J* = 6.5 Hz, 6H, 2 × $CH_3$). **$^{13}$C NMR** (101 MHz, $d_6$-DMSO) δ 154.4, 136.4, 136.2, 136.1, 135.6, 135.4, 135.4, 135.3, 135.0, 129.1, 129.0, 128.8, 128.7, 123.0, 122.9, 122.6, 68.7, 51.7, 51.6, 51.5, 49.0, 31.2, 29.3, 28.5, 28.4, 25.6, 22.1, 14.0. **HRMS** (ESI+) calc. for $C_{83}H_{100}Br_4N_{12}O_3$ $[M–2Br]^{2+}$ 816.2361; found 816.1995. **Anal.** calcd for $C_{83}H_{100}Br_6N_{12}O_3$: C, 55.59; H, 5.62; N, 9.37; found: C, 55.23; H, 5.58; N, 9.60.

**IBN-Ester-C8 (IBN-EC8)** was prepared by the general procedure from ester linker **7** and isolated as a white powder (102 mg, 0.060 mmol, 34%). **$^{1}$H NMR** (400 MHz, $d_6$-DMSO) δ 9.56–9.42 (m, 6H, ImH), 8.05–8.02 (m, 2H, PhH), 7.90–7.80 (m, 12H, ImH), 7.61–7.37 (m,

22H, PhH), 5.58–5.36 (m, 22H, $OCH_2$ + 10 × $NCH_2$), 4.18 (t, *J* = 7.0 Hz, 4H, 2 × $NCH_2CH_2$), 1.82–1.75 (m, 4H, 2 × $NCH_2CH_2$), 1.31–1.17 (m, 20H, 2 × $C_5H_{10}$), 0.85 (t, *J* = 6.5 Hz, 6H, 2 × $CH_3$). **$^{13}$C NMR** (101 MHz, $d_6$-DMSO) δ 165.2, 140.1, 136.7, 136.4, 136.2, 135.5, 135.4, 135.3, 129.9, 129.1, 129.0, 128.7, 128.5, 122.9, 122.6, 65.9, 51.6, 51.4, 49.0, 31.2, 29.3, 28.5, 28.3, 25.5, 22.1, 14.0. **HRMS** (ESI+) calc. for $C_{82}H_{98}Br_4N_{12}O_2$ $[M–2Br]^{2+}$ 801.2309; found 801.1903. **Anal.** calcd for $C_{82}H_{108}Br_6N_{12}O_7$ [M+5$H_2O$]: C, 53.14; H, 5.87; N, 9.07; found: C, 52.76; H, 5.52; N, 8.99.

**IBN-Urea-C8 (IBN-UC8)** was prepared by the general procedure from urea linker **9** and isolated as white powder (745 mg, 0.416 mmol, 75%). **$^{1}$H NMR** (400 MHz, $d_6$-DMSO) δ 9.57–9.38 (m, 6H, ImH), 7.86–7.82 (m, 12H, ImH), 7.51–7.21 (m, 24H, PhH), 6.65–6.57 (m, 2H, 2 × NH), 5.49–5.26 (m, 20H, 10 × $NCH_2$), 4.23–4.16 (m, 8H, 2 × $NHCH_2$ + 2 × $NCH_2CH_2$), 1.82–1.76 (m, 4H, 2 × $NCH_2CH_2$), 1.31–1.78 (m, 20H, 2 × $C_5H_{10}$), 0.85 (t, *J* = 6.5 Hz, 6H, 2 × $CH_3$). **$^{13}$C NMR** (101 MHz, $d_6$-DMSO) δ 158.1, 141.8, 136.4, 136.3, 135.5, 135.3, 133.0, 129.1, 129.0, 128.4, 128.5, 127.6, 127.7, 127.5, 127.4, 122.8, 122.9, 122.6, 51.9, 51.6, 51.4, 49.0, 42.3, 31.2, 29.3, 28.5, 28.3, 25.5, 22.1, 14.0. **HRMS** (ESI+) calc. for $C_{83}H_{102}Br_4N_{14}O$ $[M–2Br]^{2+}$ 815.2521; found 815.2153.

**IBN-Hemiaminal-C8 (IBN-HC8)** was prepared by the general procedure from hemiaminal linker **14** and isolated as a white powder (625 mg, 0.427 mmol, 50%). **$^{1}$H NMR** (400 MHz, $d_6$-DMSO) δ 9.74–9.35 (m, 6H, ImH), 8.00–7.77 (m, 12H, ImH), 7.52–7.45 (m, 18H, PhH), 7.19–7.12 (m, 2H, PhH), 6.26 (s, 2H, $OCH_2N$), 5.51–5.36 (m, 18H, $NCH_2$), 4.16 (t, *J* = 7.0 Hz, 4H, 2 × $NCH_2CH_2$), 1.81–1.74 (m, 4H, 2 × $NCH_2CH_2$), 1.31–1.16 (m, 20H, 2 × $C_5H_{10}$), 0.84 (t, *J* = 6.5 Hz, 6H, 2 × $CH_3$); **$^{13}$C NMR** (101 MHz, $d_6$-DMSO) δ 155.6, 136.5, 136.3, 135.6, 135.5, 135.4, 130.7, 130.4, 129.3, 129.2, 129.1, 123.0, 122.6, 116.5, 116.4, 75.2, 51.8, 51.7, 51.5, 51.4, 49.1, 31.2, 29.4, 28.6, 28.4, 25.6, 22.2, 14.1.

### *2.4. Measuring oligomer degradation by $^{1}$H NMR spectroscopy*

Sorenson's phosphate buffer (pH, 6, 7, 8) and tris buffer (pH 8) were prepared in deionized water at concentrations of 100 mM, as well as 10 mM for tris buffer solution. Stock solutions of the buffers were divided into 1 mL portions, which were freeze-dried and dissolved in 1 mL of $D_2O$. A 4-mg sample of imidazolium oligomer or polymer was dissolved in deuterated buffer solution with care taken to ensure complete solution of the compounds. The solution was stored at 25 °C in NMR tubes and $^{1}$H NMR spectra were obtained at specific time points. It was found that 128 scans were sufficient to obtain good signal-to-noise ratio at these concentrations.

Degradation of the carbonate and ester-linked compounds was observed by disappearance of the signal of the methylene protons adjacent to the carbonate or ester functional group, and/or appearance of the signal of the methylene protons adjacent to the hydroxyl group in the degradation product.

*2.5. Characterization of gels*

Gels were prepared by weighing the imidazolium oligomers directly into 4-mL glass vials and subsequently adding a known weight or volume of the solvent. The vials containing both the imidazolium and the solvent were either heated or sonicated to aid the dissolution process. The vials were left standing overnight at ambient conditions. The gel state was evaluated by the stable-to-inversion-of-a-test-tube method. The critical gelation concentration (CGC) is defined as the lowest concentration of the gelator that leads to a stable gel.

Rheological measurements were performed with a control strain rheometer (ARES G2, U.S.A) equipped with a plate-plate geometry of 8 mm diameter. Measurements were taken by equilibrating the gels at 25 °C between the plates at a gap of 1.0 mm. Strain-amplitude sweeps were performed at angular frequency of 10 rad/s. The shear storage modulus (G') and loss modulus (G") were measured at each point.

Frequency sweeps for **IBN-CC8** (4.0 wt%) and **IBN-HC8** (2.0 wt%) in alcohols were performed at strain amplitude of 2% and 5%, respectively, to ensure the linearity of viscoelasticity. The dynamic storage modulus (G') and loss modulus (G") were examined as a function of frequency from 0.1 to 100 rad/s. In addition, viscosity of the gel was also examined as a function of shear rate of 0.1– 50/s.

To test the thermal stability of the gels, the storage and loss moduli of **IBN-CC8** (4.0 wt%) and **IBN-HC8** (2.0 wt%) in alcohols were measured with a ramp 2 °C/min at 2% and 5% strain, respectively.

*2.6. Antimicrobial studies*

*2.6.1. Minimum inhibitory concentration (MIC) measurement*

*S. aureus*, *E. coli*, *P. aeruginosa*, and *C. albicans* were used as representative microorganisms to challenge the antimicrobial functions of the oligomers and their degradation products. All bacteria and fungi were stored at -80 °C, and were grown overnight at 37 °C in MHB prior to experiments. Fungi were grown overnight at room temperature (~25 °C). Subsamples of these cultures were grown for a further 3 h and diluted to give an optical density (O.D.) value of 0.07 at 600 nm (microplate reader, Tecan), which corresponded to 3

$\times 10^8$ colony forming unit (CFU) $mL^{-1}$ for bacteria and $10^6$ CFU $mL^{-1}$ for fungi (McFarland's Standard 1; confirmed by plate counts).

The oligomers were dissolved in MHB at a concentration of 4 mg $mL^{-1}$, and MIC was determined by microdilution assay [28]. Bacterial solutions (100 µL, $3 \times 10^8$ CFU $mL^{-1}$) were mixed with 100 µL of oligomer solutions (normally ranging from 4 mg $mL^{-1}$ to 2 µg $mL^{-1}$ in serial two-fold dilutions) in 96-well plate. The plates were incubated at 37 °C for 24 h with a shaking speed of 300 rpm. The MIC measurement against *Candida albicans* was similar to bacteria except that the fungi solution was $10^6$ CFU $mL^{-1}$, and the plates were incubated at room temperature.

The MIC was taken as the concentration of the antimicrobial oligomer at which 50% microbial growth was observed with the microplate reader. Phosphate-buffered saline (PBS) solution containing only microbial cells were used as the negative control (i.e. 100% microbial growth). The assay was performed in four replicates, and the experiments were repeated at least two times.

*2.6.2. Resistance studies*

The method was modified from that of Fukushima *et al.* [31]. Drug resistance was induced by treating *S. aureus* repeatedly with degradable oligomers. MICs of the oligomers were determined against *S. aureus* using the broth microdilution method. Next, serial passaging was initiated by transferring bacterial suspension grown at sub-MIC of the oligomers (1/2 of MIC at that passage) for another MIC assay. After 24 h of incubation, cells grown at sub-MIC of the tested compounds/antibiotics were once again transferred and assayed for MIC. The MIC against *S. aureus* was tested for 16 passages.

Drug-resistant behavior of *S. aureus* was evaluated by recording the changes in the MIC normalized to that of the first passage. Conventional antibiotic vancomycin was used as the control.

*2.6.3. Time kill kinetics*

The microbes were treated with oligomers at 4MIC concentration, and samples were taken out of each well at different intervals. 100 µL of cell suspension was removed, rescued by a series of 10-fold dilutions with growth medium. For plating, 100 µL of the diluted samples was spread on growth medium agar plates, and colonies were counted after overnight incubation at 37 °C.

*2.6.4. Monitoring the changes in antimicrobial activity during degradation*

The changes in antimicrobial activity during degradation were monitored by measuring MIC during the process. The degradable oligomers were dissolved in Sorenson's phosphate buffers (pH 6, 7 and 8; 100 mM), tris buffer (pH 8; 100 mM), and saline. Stock solutions were 4 mg/ml in concentration. The solution was stored at 25 °C, and the MICs against *E.coli* and *S. aureus* were measured at different intervals.

*2.7. Hemolysis assay*

Fresh rat red blood cells (RBCs) were diluted with PBS buffer to give an RBC stock suspension (4 vol% blood cells). 100-µL aliquots of RBC suspension were mixed with 100 µL of oligomer solutions (ranging from 4 mg $mL^{-1}$ to 2 µg $mL^{-1}$ in serial two-fold dilutions in PBS). After 1 h of incubation at 37 °C, the mixtures were centrifuged at 2000 rpm for 5 min. Aliquots (100 µL) of the supernatant were transferred to a 96-well plate. Hemolytic activity was determined as a function of hemoglobin release by measuring the absorbance of the supernatant at 576 nm using the microplate reader. A control solution that contained only PBS was used as a reference for 0% hemolysis. Absorbance of red blood cells lysed with 0.5% Triton-X was taken as 100% hemolysis. The data were expressed as mean and S.D. of four replicates, and the tests were repeated two times.

$$\% \text{ Hemolysis} = \frac{OD576\,(oligomer) - OD576\,(PBS)}{OD576\,(Triton{-}X) - OD576\,(PBS)}\ X\ 100$$

*2.8. Scanning electron microscopy (SEM) of gel and bacteria*

The morphologies of the organogel microstructure were examined with field emission scanning electron microscopy (FESEM) (JEOL JSM-7400F) operated at an accelerating voltage of 3 keV. The gels were dried via supercritical drying, and stored under anhydrous conditions, either in a glovebox or a desiccator prior to imaging.

Bacterial cells ($3\times10^8$ CFU/ml) grown in MHB with or without the oligomers at 4MIC for 2 min were collected and centrifuged at 3000 rpm for 5 min. The precipitates were washed twice with PBS buffer. Next, the samples were fixed with glutaraldehyde (2.5%) for 2 h, followed by washing with DI water. Dehydration was performed using a series of ethanol/water solutions (35%, 50%, 75%, 90%, 95% and 100%). The dehydrated samples were mounted on copper tape. After drying for 2 days, the samples were further coated with platinum for imaging with JEOL JSM-7400F field emission scanning electron microscope (Japan) operated at an accelerating voltage of 3 keV.

*2.9. In vitro cytotoxicity study*

The effects of the oligomers and their degradation products on cell viability were examined using CellTiter-Glo® Luminescent Cell Viability Assay (Promega). Primary human dermal fibroblasts (HDF, ATCC PCS-201-012) were cultured in Dulbecco's Modified Eagle's Medium (DMEM) supplemented with 10% fetal bovine serum (Life Technologies) and 100 IU/mL penicillin-streptomycin (Life Technologies) and maintained at 37 °C in a 5% $CO_2$ incubator. Cells were allowed to expand to 80–90% confluence before passaging with 0.05% trypsin-ethylenediaminetetraacetic acid (EDTA, Life Technologies). Cells were seeded onto 96-well plates at ~$10^4$ cells/well and incubated for 2 days. Oligomers in DMEM were diluted with culture medium to give final nanoparticle concentrations of 2, 4, 8, 16, 31, 62.5, 125, 250, 500, 1000 and 2000 μg/mL. The media in the wells were replaced with 100 μL of the pre-prepared oligomer solutions. The plates were then returned to the incubator, and maintained in 5% $CO_2$ at 37 °C for 24 h. 100 μL of CellTiter-Glo® Reagent was added to each well for cell lysis. The plates were incubated at room temperature for 10 min to stabilize the signal, and luminescence was measured with a microplate reader (Tecan Safire). The cell viability was expressed as the ratio of the number of viable cells with treatment to that without treatment. Experiments were conducted in triplicates, and consistent results were obtained.

*2.10. Animal studies*

Male C57BL/6Jinv mice, 6–8 weeks old, were obtained from InVivos Pte Ltd, Singapore. The mice were randomly grouped. 5 mice were used in each group. All the animals were maintained on a 12-h light/dark cycle with access to food and water *ad libitum*. All animal procedures were approved by Institutional Animal Care and Use Committee, Biological Resource Center, Singapore (protocol number: 140980).

*2.10.1. Skin toxicity test*

*In vivo* dermal compatibility tests were conducted to confirm that the oligomer solutions were not skin toxic. 5 groups each containing 2 mice were used for this study. Before the test, mice were anesthetized by *i.p.* injection with pentobarbital (50 mg/kg b.w.). The skin on the back and the neck of each mouse (~ 2 cm × 2 cm) was shaved with an electric razor. In groups 1, 2 and 3, aqueous solution of the oligomers (80 μg/mL; 0.2 mL) was applied evenly onto the shaved back of each mouse. In groups 4 and 5, water solution

and vancomycin solution were applied for the positive and negative controls, respectively. All the mice were treated once daily. After 7 days, the mice were sacrificed and the treated skin tissues were collected for histological examination. The sample was fixed in paraformaldehyde (4%) and embedded in paraffin. Paraffin sections (4 μm-thick) were cut and stained with hematoxylin and eosin. Images of the stained tissues were captured with an Olympus IX-83 (Tokyo, Japan) inverted microscope.

*2.10.2. In vivo antimicrobial activity*

The full-thickness scalpel wounds were created as described in [32]. The mice were anesthetized via intraperitoneal injection of sodium pentobarbital solution (350 mg/kg). The skin on the back and the neck of the mice was shaved with an electric razor. Three parallel 8-mm full-thickness scalpel cuts were made with scissors into the dermis. The wounds were inoculated with 30 μL of *S. aureus* ($1.1 \times 10^8$ CFU/mL, based on plate counts) with a micropipettor. 1 h after *S. aureus* inoculation, the infected wounds were treated with the degradable oligomers (30 μL; 80 μg/mL in aqueous solution), followed by daily application thereafter for 4 days. Mice with their infected wounds treated with sterile water were used as the negative controls. Mice applied with vancomycin at the same dosage as oligomers (80 μg/mL in aqueous solution) were used as the positive controls.

After 4 days of consecutive treatment with degradable oligomers, all mice were killed with $CO_2$ on the following day. The wounds were excised aseptically, and then homogenized in 1 mL of PBS. Viable bacteria in PBS solution were counted by preparing 10-fold serial dilutions, and culturing the diluted systems on Lysogeny broth (LB) agar for 24 h at 37 $^oC$, after which CFUs were counted manually. Four animals in each group were tested for bacterial counts. The other mouse was killed, and the wound was used for histological analysis.

*2.11. Statistical analysis*

Data were expressed as means ± standard deviation of the mean (S.D.). Student's *t*-test was used to determine significance among groups. A difference with $P < 0.05$ was considered statistically significant.* $p < 0.05$, ** $p < 0.01$, *** $p < 0.001$.

## 3. Results and discussion

*3.1. Material design and synthesis*

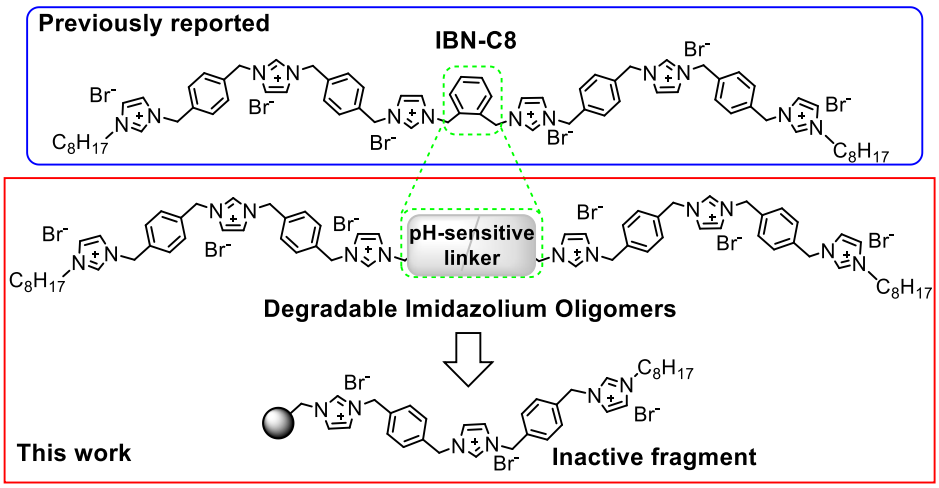


**Scheme 1.** Design of self-degradable imidazolium oligomers.

For the design of new imidazolium antimicrobial materials, degradable linkers were incorporated within the structures of antimicrobial imidazolium oligomers in a manner that retained the oligomer's bactericidal properties, but upon degradation leaft inactive fragments that would not induce antibiotic resistance development. We have learned from our previous work on antimicrobial imidazolium oligomers that a minimum of four imidazolium units per oligomer was required for antimicrobial activity [21]. Hence, the arrangement of imidazolium units along the main-chain (Scheme 1) was preserved, while we replaced the central *o*-xylylene linker in **IBN-C8** with a degradable functional group [27]. The degradable functional groups took the form of carbonate, ester, urea or hemiaminal linkers. Novel degradable imidazolium oligomers **IBN-CC8**, **IBN-EC8**, **IBN-UC8** and **IBN-HC8** were assembled by combining di-imidazole units containing degradable linkers (compounds **3**, **7**, **9** and **14**, Scheme 2) with two equivalents of fragment **16** containing the $C_8$-alkyl chain terminal group.

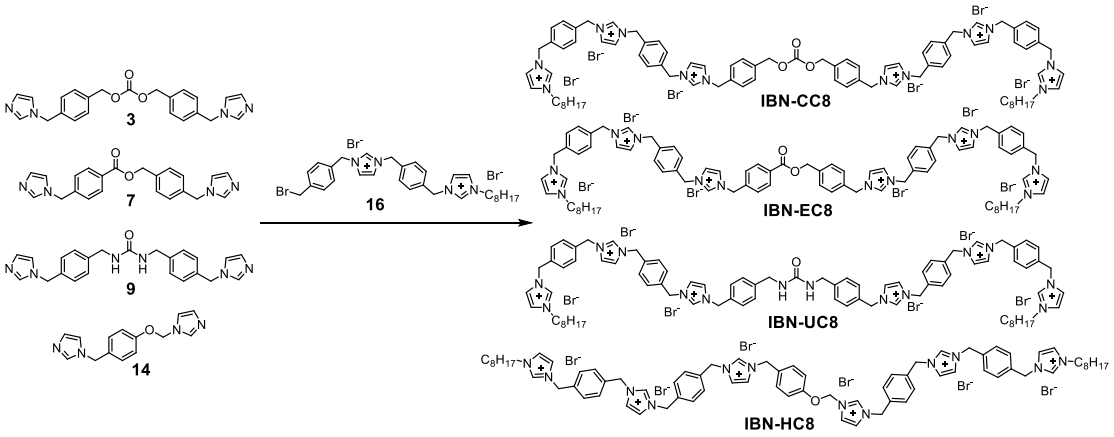

**Scheme 2.** Synthetic schemes of self-degradable imidazolium oligomers.

The newly synthesized degradable oligomers, possessing the same long alkyl chain terminal groups as **IBN-C8**, were found to be similarly capable of self-assembly in simple straight chain alcohol solvents frequently used in disinfection applications (Table S1, Supporting Information). **IBN-HC8**, in particular, showed good gelation ability in ethanol, *n*-propanol and *n*-butanol with CGCs in the range of 0.5-1.5 wt% (Figure 1a). Rheological characterization (Supporting Information Figures S1–4) and SEM images on the **IBN-HC8** xerogel (Figure 1b) were consistent with fluid matrix organogels comprising fibrillar networks of amphiphilic oligomer structures that were intertwined in the solvent mix, thereby trapping solvent molecules.

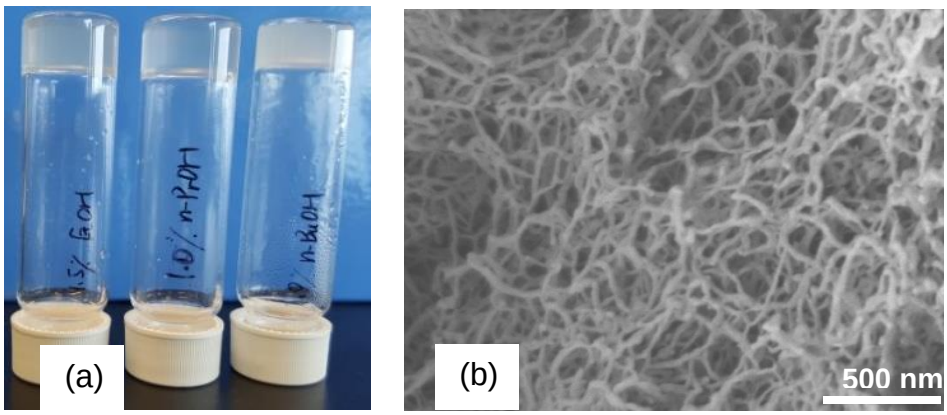


**Figure 1.** Self-degradable oligomers self-assembled to form gels in simple straight chain alcohol solvents. **(a)** Photograph of **IBN-HC8** gels formed in EtOH (1.5%), *n*-PrOH (1.0 wt%), and *n*-BuOH (1.0 wt%). **(b)** SEM image of **IBN-HC8** gel in EtOH (5 wt%).

*3.2. Degradation profiles*

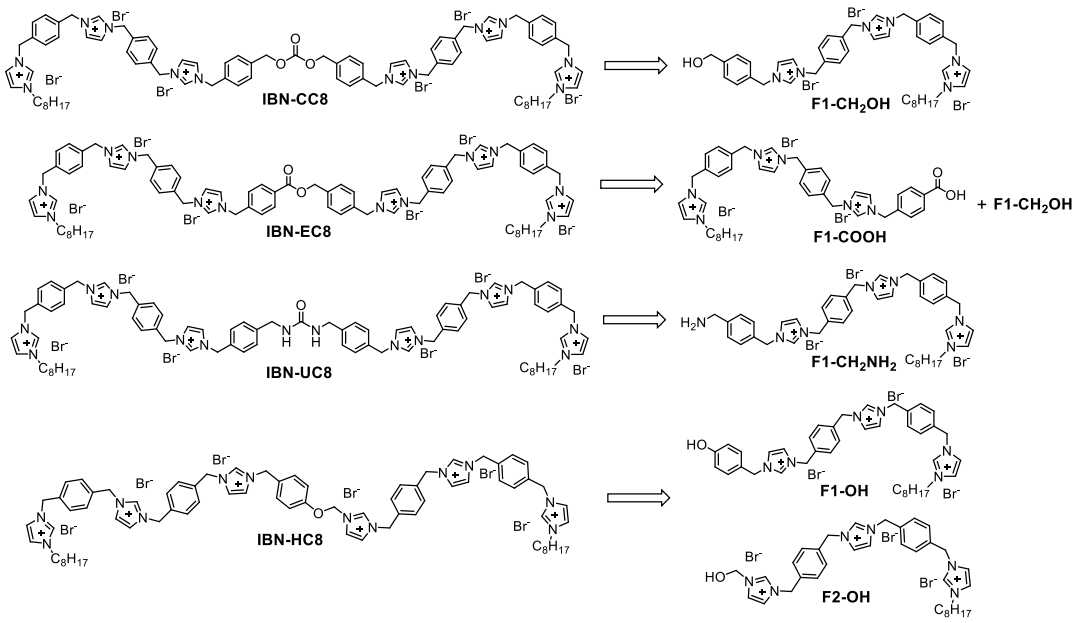


**Scheme 3.** Degradation products of imidazolium oligomers.

The potential degradation products of oligomers **IBN-CC8**, **IBN-EC8**, **IBN-UC8** and **IBN-HC8** are listed in Scheme 3. The degradation profile of each linker was investigated under pH 6–8 by analyzing the $^{1}$H NMR spectra of the oligomers stored in buffered $D_2O$ over time (Figures 2 and S5–6). Carbonate-linked oligomer (**IBN-CC8**) was observed to degrade in a pH-sensitive manner. The half-life of **IBN-CC8** in Sorenson's phosphate buffer was 18 days at pH 8, 90 days at pH 7, and > 90 days at pH 6 (Figure 2a). In addition, the degradation at pH 8 was accelerated in tris buffer solution and slowed down when the buffer concentration was decreased (Figure 2b). **IBN-CC8** was stable under mildly acidic conditions, and degraded under neutral and basic conditions. This property is desirable as bacterial infection generally reduces the pH of the infection site to 6 and below [33]. The carbonate-linked material would remain active in areas of bacterial infection, and degrade gradually in the absence of bacterial infection. Similarly, oligomer **IBN-EC8** with an ester linkage degraded at pH 8 in Sorenson's phosphate buffer with a half-life of 17 days (Figure 2c). However, this compound was relatively stable under neutral and acidic conditions. Urea and hemiaminal oligomers, **IBN-UC8** and **IBN-HC8**, were not significantly degraded in pH 6-8 buffered solutions under ambient conditions (Supporting Information Figure S6).

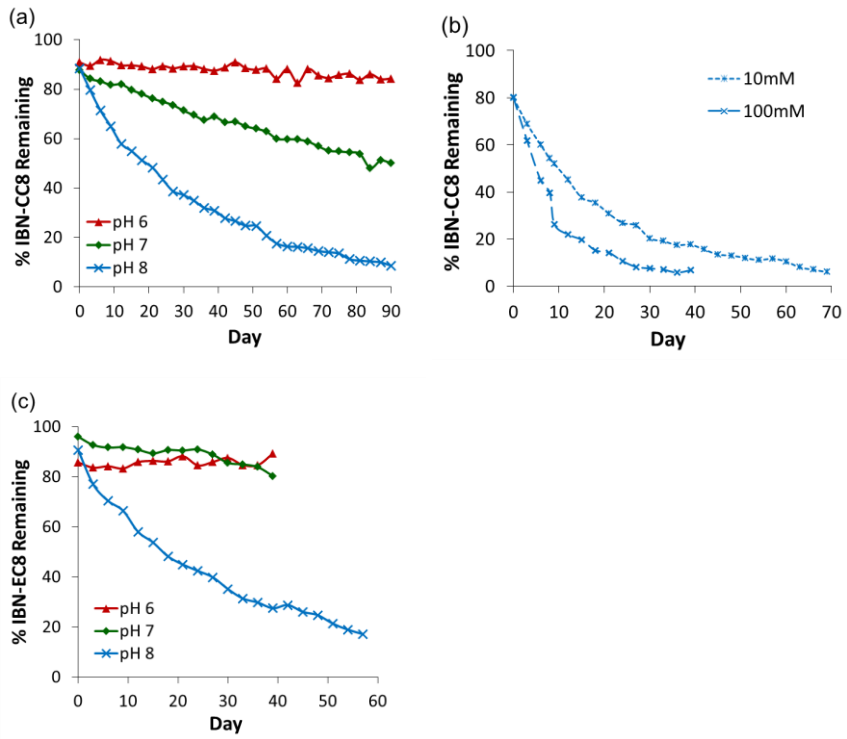


**Figure 2. IBN-CC8** and **IBN-EC8** degrade at different rates in buffered solutions with different pH values (4 mg/ml). (a) **IBN-CC8** in Sorenson's phosphate buffer (pH 6, 7, 8; 100 mM). (b) **IBN-CC8** in tris buffer solution (pH 8; 10 mM, 100 mM). (c) **IBN-EC8** in Sorenson's phosphate buffer (pH 6, 7, 8; 100 mM).

*3.3. Evaluation of antimicrobial properties*

The antimicrobial activities of the novel imidazolium oligomers and their degradation products were evaluated against four clinically relevant microbes, *S. aureus*, *E. coli*, *P. aeruginosa*, and *C. albicans*. The MIC values are presented in Table 1. All four oligomers are generally active against these microbes. **IBN-CC8** and **IBN-EC8** were the most potent materials among the four oligomers, and displayed antimicrobial activity that was similar to or slightly weaker than the parent **IBN-C8** oligomer.

**Table 1.** Antimicrobial activities ($MIC_{50}$), hemolytic activities ($HC_{10}$) and cytotoxicities ($IC_{50}$) of the oligomers and their degradation products.

| Entry | Compound | $MIC_{50}$ [a] (μg/mL) | | | | $HC_{10}$ [b] (μg/mL) | $IC_{50}$ [c] (μg/mL) |
|---|---|---|---|---|---|---|---|
| | | *E. coli* | *S. aureus* | *P. aeruginosa* | *C. albicans* | | |
| **1** | **IBN-CC8** | 8 | 8 (8[d]) | 125 | 31 | > 2000 | 101 |
| **2** | **IBN-EC8** | 8 | 8 (8[d]) | 31 | 125 | 1000 | 124 |
| **3** | **IBN-UC8** | 8 | 8 (8[d]) | 500 | 62 | 2000 | 140 |
| **4** | **IBN-HC8** | 8 | 8 (8[d]) | 125 | 125 | > 2000 | 805 |
| **5** | **F1-$CH_2OH$** | 62 | 62 | 1000 | 250 | > 2000 | 591 |
| **6** | **F1-COOH** | 31 | 62 | > 2000 | 500 | > 2000 | 549 |
| **7** | **F1-$CH_2NH_2$** | 16 | 125 | 250 | 62 | 1000 | 155 |
| **8** | **F1-OH** | 31 | 16 | 1000 | 500 | > 2000 | 478 |
| **9** | **IBN-C8** | 8 | 4 | 16 | 16 | > 2000 | 125 |
| **10** | Vancomycin | - | 2 (8[d]) | - | - | > 2000 | > 2000 |

[a] MIC against $3 \times 10^8$ CFU $mL^{-1}$ of bacteria or $10^6$ CFU $mL^{-1}$ of fungi. [b] $HC_{10}$ was taken as oligomer concentration at which the oligomers cause 10% hemolysis. [c] Cytotoxicity against human primary dermal fibroblasts after 24 h incubation. $IC_{50}$ was taken as the oligomer concentration at which the oligomers cause less than 50% cell viability. [d] MIC against $3 \times 10^8$ CFU $mL^{-1}$ of passage-selected vancomycin-intermediate *Staphylococcus aureus*, which was obtained in the resistance study after 16 passages under sub-MIC levels of vancomycin.

The killing kinetics of **IBN-CC8**, **IBN-EC8** and **IBN-C8** were studied against *E. coli*. The CFUs of *E. coli* after treatment with 62 μg/mL of imidazolium compounds for various periods are shown in Figure 3. The carbonate and ester-linked imidazolium oligomers displayed fast killing properties that were comparable to the first generation compound **IBN-C8**. More than 99% killing was observed within 2 min for all three compounds at 62 μg/mL. For **IBN-CC8**, total loss of cell viability was observed within 3 h after exposure.

The morphological changes in bacteria after treatment with these oligomers were examined with SEM. As shown in Figure 4, the cell walls of both *E.coli* and *S. aureus* were disrupted and subsequently dissolved following exposure to **IBN-CC8**, **IBN-EC8** or **IBN-HC8** for just 2 min.

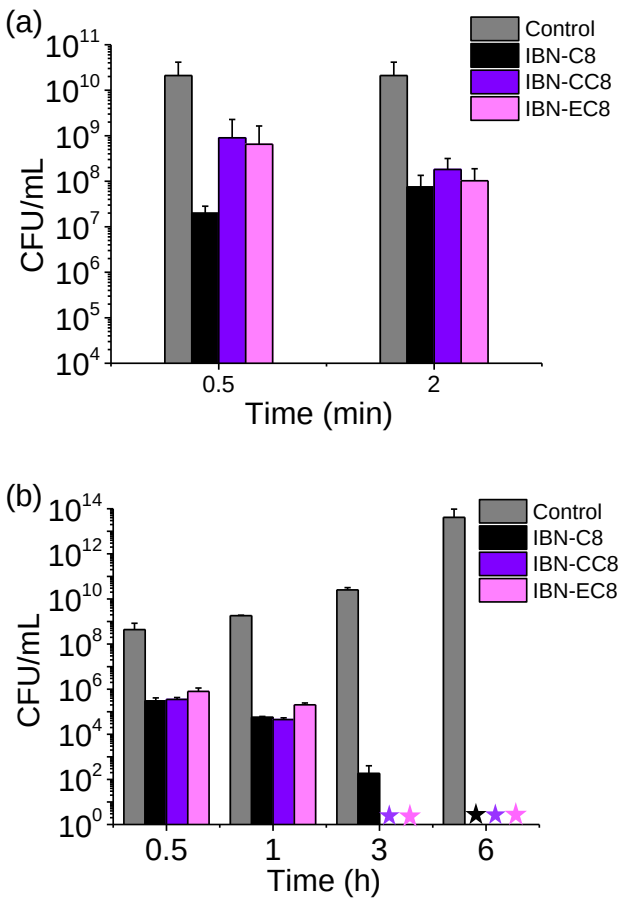


**Figure 3.** Killing efficiency for **IBN-C8**, **IBN-CC8** and **IBN-EC8** at 62 μg/mL against *E. coli* after **(a)** short and **(b)** long incubation times. Star indicates that no colony was observed. The data are expressed as mean ± S.D. of triplicates.

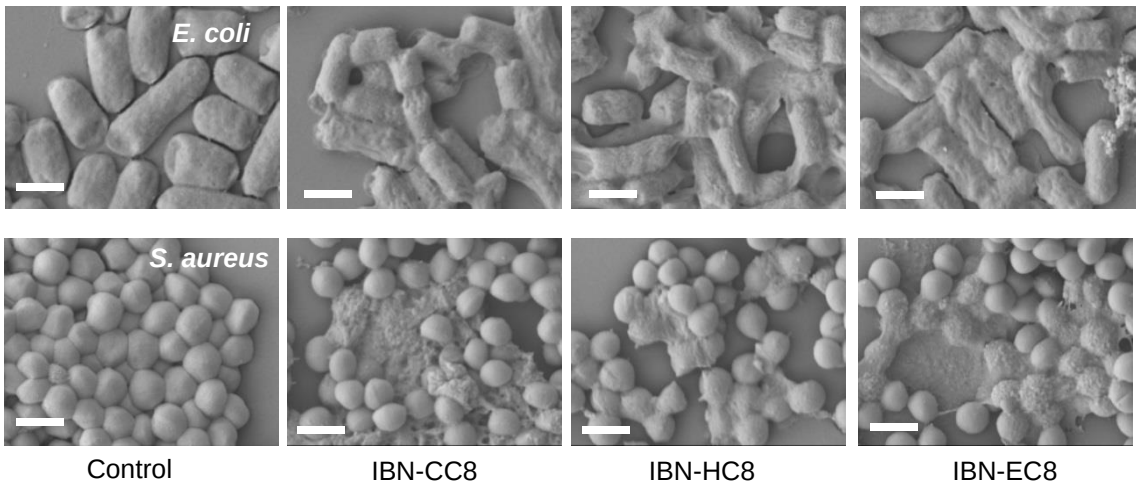


**Figure 4.** SEM images of *E. coli* and *S. aureus* treated with degradable oligomers (62 μg/mL) for 2 min. Bacteria grown in MHB were used as controls. Cell walls were disrupted and dissolved after exposure to the oligomers. Scale bars represent 1 μm.

Over the course of degradation, conversion of the active oligomers to less active degradation product(s) would be expected to be reflected in the changes in MIC values for the degrading oligomer mixtures. To determine if this was indeed the case, **IBN-CC8** and **IBN-EC8** were dissolved in buffer solutions, and the MIC values of the buffered oligomer solutions against *E. coli* and *S. aureus* were monitored over time (Figures 5 and S7–8).

In Sorenson's phosphate buffer at pH 8, the MIC of **IBN-CC8** against *E. coli* doubled from 32 μg/mL at day 0 to 64 μg/mL after 30 days (Figure 5a). At pH 7, the MIC of **IBN-CC8** against *E. coli* doubled after 32 days from 16 μg/mL to 32 μg/mL, and doubled again at day 130 to 64 μg/mL. And at pH 6, the MIC of **IBN-CC8** against *E. coli* remained at 16 μg/mL for 110 days, after which it doubled to 32 μg/mL. Similar trends were observed for the MIC values of **IBN-CC8** in phosphate buffer (pH 6, 7 and 8) when tested against *S. aureus* (Figure 5b). The antimicrobial activity of **IBN-CC8** in tris buffer (pH 8) against *E. coli* showed the most rapid decay, with MIC increasing from 8 μg/mL at day 0 to 32 μg/mL at day 3, and 250 μg/mL at day 21. The MIC of **IBN-CC8** in the same buffer against *S. aureus* quadrupled from 8 μg/mL to 32 μg/mL in 9 days, after which it remained constant for 35 more days. On the whole, these MIC changes were in good agreement with the degradation profile of **IBN-CC8** in different pH buffer solutions (Figure 2).

Oligomer **IBN-EC8** also exhibited diminishing antimicrobial activity when stored at pH 8 in Sorenson's phosphate buffer. MIC of **IBN-EC8** against *E. coli* and *S. aureus* doubled after 35 and 20 days, respectively, and remained unchanged until 70 days at pH 8 (Figures S8). At pH 7, change of MIC was only observed at 70 days when tested against *E. coli*. Under acidic conditions, the MICs of **IBN-EC8** against *E. coli* and *S. aureus* did not change over 70 days. These results support the degradation profiles obtained from NMR analysis.

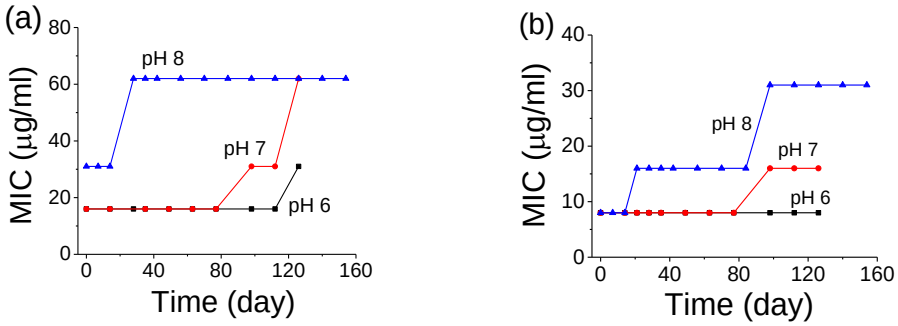


**Figure 5.** Changes in MIC for **IBN-CC8** stored in Sorenson's phosphate buffer (pH 6, 7 and 8) against **(a)** *E. coli* and **(b)** *S. aureus*.

*3.4. Drug resistance development study*

The potential for bacterial cells to develop resistance following multiple exposure to oligomers **IBN-CC8**, **IBN-EC8**, **IBN-HC8** and **IBN-UC8** and vancomycin was investigated by serial passage of *S. aureus* under sub-MIC levels of each oligomer. After each passage, MIC values were determined for the respective oligomers against the cultured bacteria cells. As shown in Figure 6, *S. aureus* cultured in a sub-MIC concentration of vancomycin was the first to form resistance (after just five passages). By the 14$^{th}$ passage, it took four times the original concentration of vancomycin to inhibit bacterial growth. Bacterial cells grown in the presence of **IBN-HC8** started developing resistance to the oligomer after eight passages. In contrast, bacterial cells grown in the presence of **IBN-CC8**, **IBN-EC8** and **IBN-UC8** did not acquire resistance to the oligomers over the entire study (i.e. 16 passages). These results demonstrated a much slower rate of resistance development when *S. aureus* was treated with the carbonate-, ester- and urea-linked imidazolium oligomers, as compared with vancomycin.

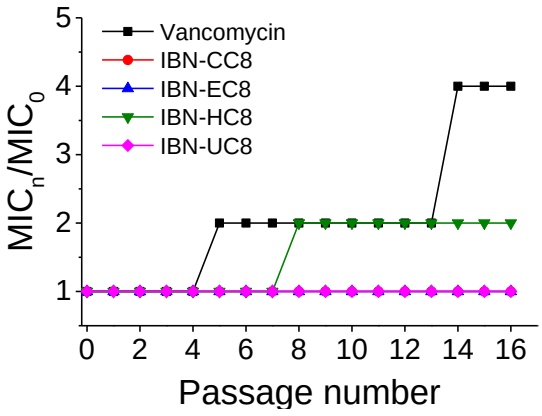


**Figure 6.** Changes in MICs of **IBN-CC8**, **IBN-EC8**, **IBN-HC8**, **IBN-UC8** and vancomycin against *S. aureus* cultured in the presence of sub-MIC levels of the respective antimicrobial compound.

*3.5. Biocompatibility*

For biomedical applications, it is important for the antimicrobial compounds to be compatible with mammalian cells. Hemolysis assay is commonly used to evaluate the toxicity of antimicrobial compounds by measuring the hemoglobin release by ruptured red blood cells (RBCs). Hemolytic behavior of the oligomers and their degradation products were evaluated over a range of concentrations (Table 1).

All the oligomers did not induce noticeable hemolysis at their respective MIC. For **IBN-CC8** and **IBN-HC8**, no hemolysis was observed even at 2000 μg/mL, the highest concentration tested. Considering their high antimicrobial activity, these oligomers qualified as active and non-toxic compounds with high selectivity for a wide range of pathogenic microbes over mammalian cells. In addition, the degradation product of **IBN-CC8**, **F1-$CH_2OH$**, is essentially non-toxic ($HC_{10}$ >2000 μg/mL) and less active against pathogenic microbes. These properties position **IBN-CC8** as a promising antimicrobial material with optimum activity and degradability.

To evaluate their potential as topical antimicrobials, we measured the cytotoxicity of these oligomers and their degradation products against human primary dermal fibroblasts after 24 h of incubation. As shown in Table 1, **IBN-HC8** has the highest $IC_{50}$ value, indicating the lowest cytotoxicity. Although **IBN-CC8** has a lower $IC_{50}$ value than vancomycin, its degradation to markedly less cytotoxic **F1-$CH_2OH$** indicated that it could still be suitable for topical applications**.**

**IBN-EC8** and **IBN-UC8** caused 10% haemoglobin leakage from RBCs at 1000 and 2000 μg/mL, and reduced dermal fibroblast viability to < 50% at concentrations below 150 μg/mL. **IBN-EC8** would still be an attractive antimicrobial given its wide therapeutic window and degradation to non-hemolytic and mildly cytotoxic products, **F1-$CH_2OH$** and **F1-COOH**. In the case of **IBN-UC8**, the anticipated degradation product **F1-$CH_2NH_2$** displayed relatively high antimicrobial activity and cytotoxicity as compared to the parent oligomer. Thus, it was deemed to be an unsuitable candidate for further studies.

Oligomer solutions (80 μg/mL) were then tested for dermal compatibility to determine if they were safe for skin application. After 7 consecutive days of treatment, the mice in the oligomer-treated groups did not show any sign of irritation. Histological study was used to evaluate cellular integrity, changes in tissue structure and inflammation in epidermis, dermis and subcutaneous levels. No significant accumulation of inflammatory cells was observed for all the treated groups (see Figure 7). The overall structure and cellular integrity of the oligomer-treated skin were similar to that of water-treated skin. Taken together, these results indicated that **IBN-CC8**, **IBN-HC8** and **IBN-EC8** solutions of 80 μg/mL were biocompatible, and this concentration was employed for the topical treatment of bacteria-infected wounds in mice.

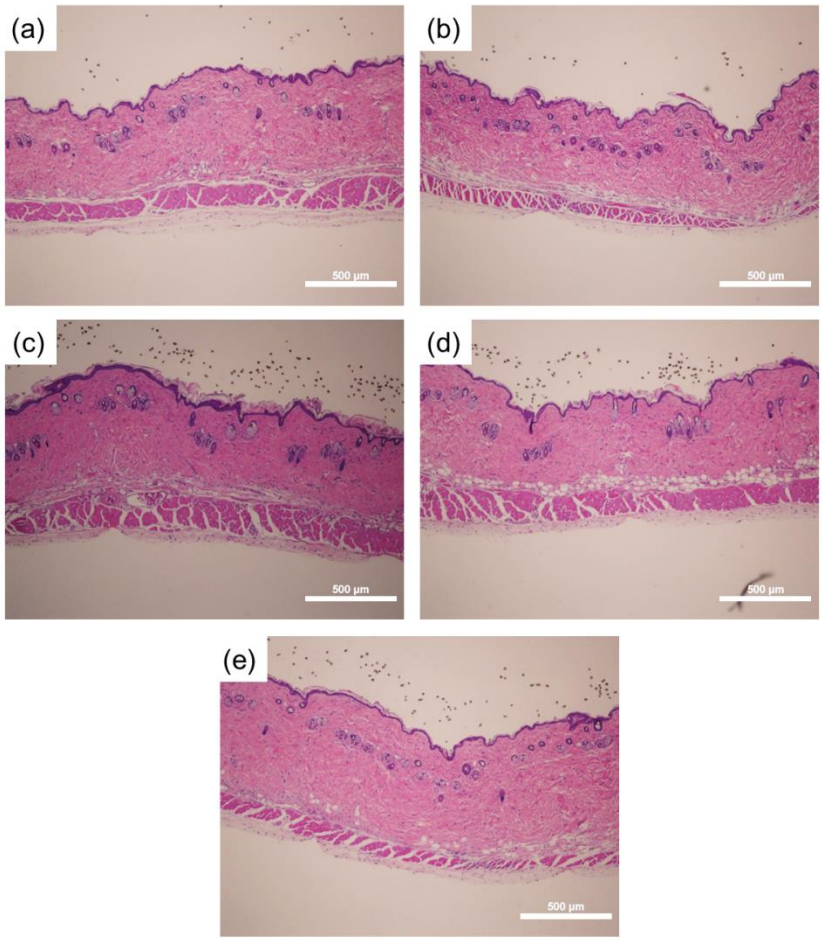


**Figure 7.** Histological evaluation of mouse skin after daily treatment with 200 µl of **(a)** water, **(b)** vancomycin (80 µg/mL), **(c) IBN-CC8** (80 µg/mL), **(d) IBN-HC8** (80 µg/mL) and **(e) IBN-EC8** (80 µg/mL) for 7 days. Scale bars represent 500 µm.

*3.6. Efficacy of degradable oligomers in topical treatment of S. aureus infected wound*

To evaluate the *in vivo* bactericidal activity of the oligomers, a *S. aureus* skin wound infection model was adopted. Briefly, three full-thickness scalpel cuts on the back of mice were inoculated with *S. aureus.* The infected open wounds were then treated with daily applications of the degradable oligomers for four consecutive days. Wounds treated with sterile water were used as negative controls, while vancomycin-treated wounds were employed as positive controls. After treatment, the number of *S. aureus* cells recovered from the infected wounds was determined after overnight culture of homogenized lesioned skin. Cross-sections of the wounds at maximum size were obtained for hematoxylin and eosin (H&E) staining to evaluate wound healing behavior.

All the mice survived the 4-day experiment. The appearances of the *S. aureus*-inoculated wounds immediately after creation and 4 days after treatment are shown in Figure

8. Significant differences between the water-treated wounds and vancomycin- or oligomer-treated wounds were observed. Water-treated wounds were twice the size of the vancomycin-treated and oligomer-treated wounds (Figure 9a), illustrating that the wound sizes were significantly reduced after treatment with vancomycin or oligomers. There was no statistical difference between the lesion sizes of oligomer-treated wounds and vancomycin-treated wounds.

The antimicrobial efficacy of each treatment was evaluated based on the number of viable *S. aureus* recovered from the wounds after 4 days (Figure 9b). The number of *S. aureus* recovered from oligomer-treated wounds was significantly reduced compared to the water-treated control (80–90% reduction), and was comparable to that obtained for vancomycin-treated wounds.

A primary indicator of successful cutaneous wound healing is reforming a continuous layer of cornified epidermis to restore the barrier capacity of skin. Images of H&E-stained wounds after 4 days of treatment are shown in Figure 10. For the wounds treated with water, the three cuts fused into a large wound. Minimal re-epithelialization was observed, leaving most of the wound exposed. Faster re-epithelialization was observed for vancomycin- and oligomer-treated wounds. The leading edges of the epidermis were immigrating inwards to close the wounds. Specifically, a continuous epidermis and a visible layer of stratum corneum appeared on wounds treated with vancomycin, **IBN-CC8** and **IBN-HC8**, indicating complete re-epithelialization. For **IBN-EC8**-treated wound, the newly regenerated epidermis was several layers thick, and thinner than the unwounded epidermis. These histological findings were consistent with the wound appearances in Figure 8. The results suggested that accelerated bacteria clearance and wound healing could be achieved by topical application of the degradable oligomers.

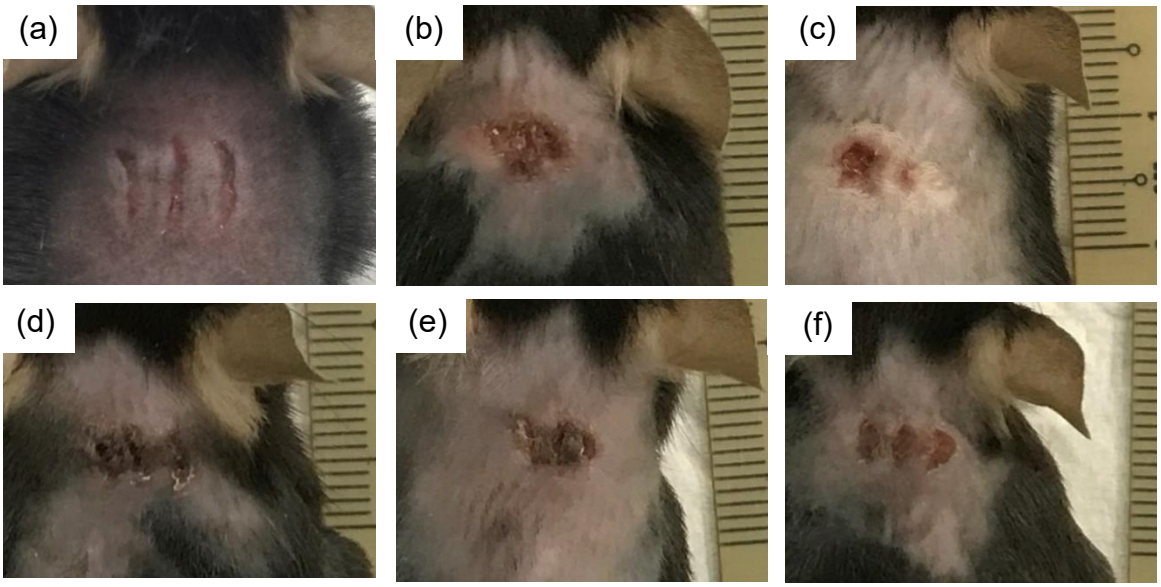


**Figure 8.** Images of the wounds on **(a)** day 0 after inoculation of *S. aureus*, and on day 5 after treatment with **(b)** $H_2O$, **(c)** vancomycin, **(d) IBN-CC8**, **(e) IBN-HC8** and **(f) IBN-EC8**.

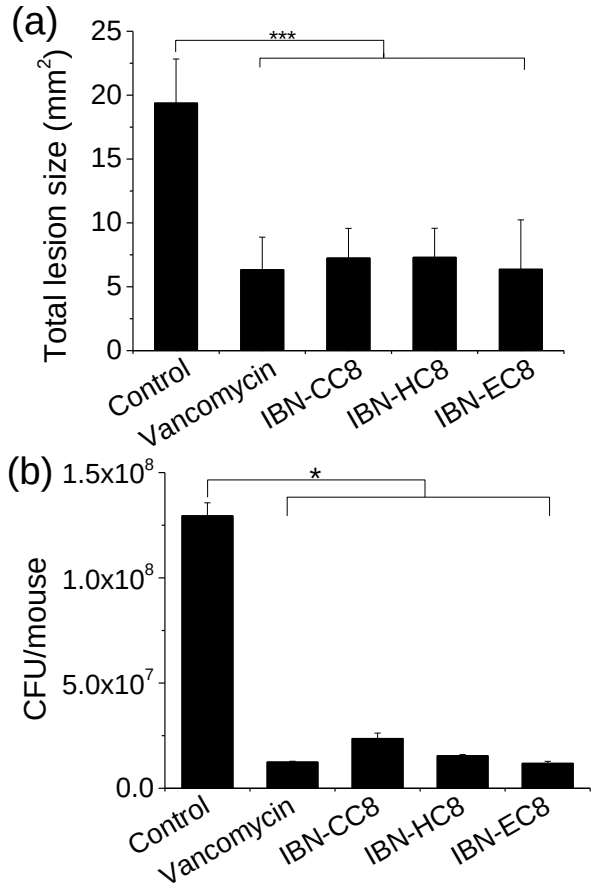


**Figure 9. (a)** Changes in wound area after 4 days of treatment with $H_2O$ (control), vancomycin and self-degradable oligomers. **(b)** Microbiology counts (CFU) of *S. aureus* in the cut wounds of mice after treatment with $H_2O$ (control), and with 80 µg/ml of vancomycin

and oligomers. The data are expressed as mean ± S.D. of quadruplicates. * $p < 0.05$; *** $p < 0.001$.

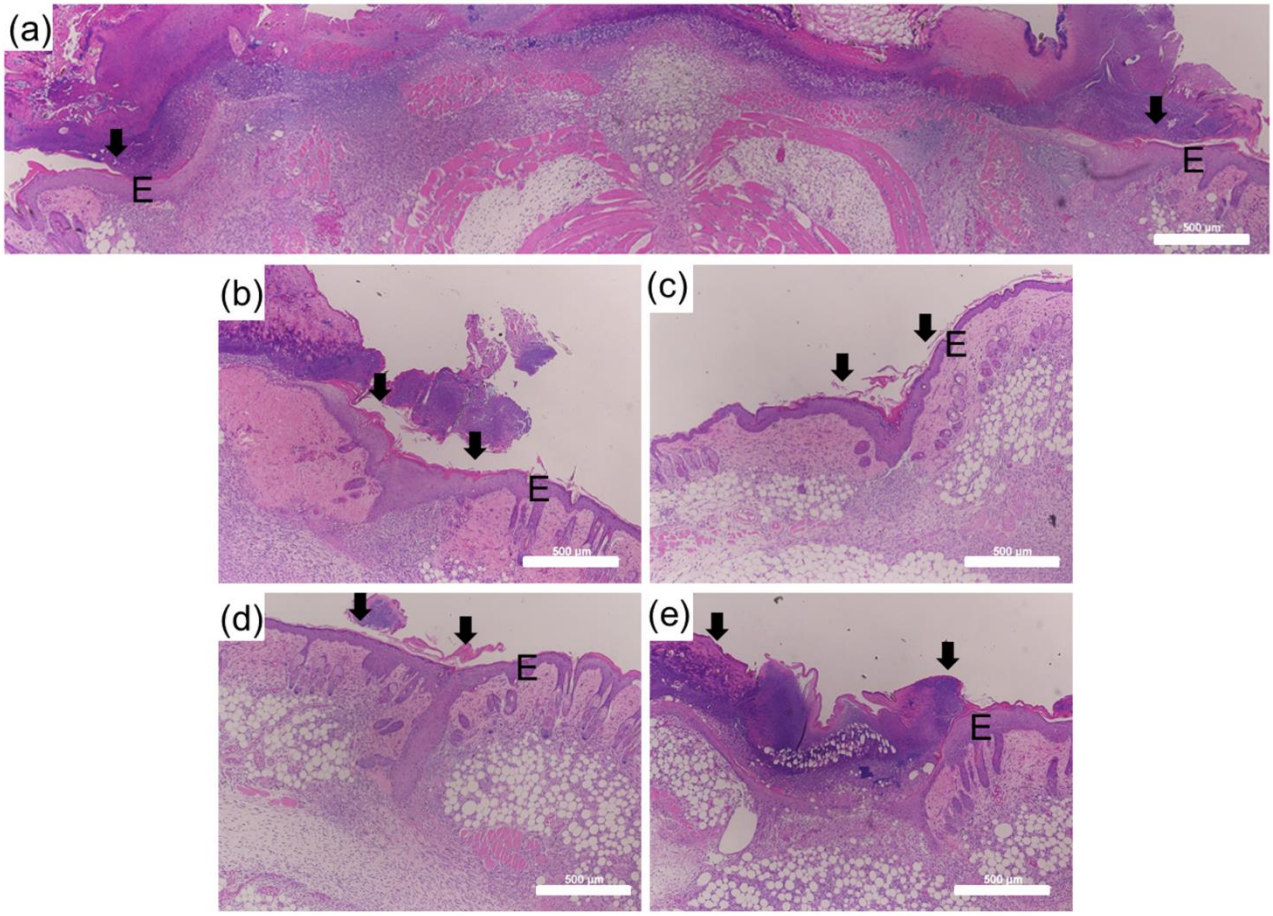


**Figure 10.** Histological analysis of cut wounds in mouse skin after 4 days of daily application of **(a)** water, and 80 µg/mL of **(b)** vancomycin, **(c) IBN-CC8**, **(d) IBN-HC8**, and **(e) IBN-EC8**. Arrow points to the edge of the wound. E = Epidermis. Scale bars represent 500 µm.

## 4. Conclusion

A new series of imidazolium oligomers incorporating self-degradable linkers has been developed. The new imidazolium materials retained the excellent antimicrobial activity of the previous generation of materials against a broad range of microbes. **IBN-CC8** and **IBN-EC8** possessed tuneable degradability and biocompatibility. They also left no active residue after treatment for potential secondary contamination and drug resistance development. When applied as topical antimicrobials, these oligomers accelerated bacteria clearance and wound healing, making them promising eco-friendly antimicrobial materials for topical wound treatment and personal care.

**Acknowledgements**

This work was supported by the Institute of Bioengineering and Nanotechnology and NanoBio Lab, Biomedical Research Council, Agency for Science, Technology and Research.

**Research data is available in Appendix A. Supplementary material**

**References**

1. J. O'Neill, Review on antimicrobial resistance. Antimicrobial resistance: Tackling a crisis for the heath and wealth of nations, 2014
2. S.B. Levy, B. Marshall, Antibacterial resistance worldwide: Causes, challenges and responses, Nature Medicine 10 (2004) S122-S129.
3. World Health Organization, Fact sheet, Antimicrobial resistance. http://www.who.int/mediacentre/factsheets/fs194/en/ "reports of bacterial infections by strains resistant to all existing drugs"
4. B. Perichon, P. Courvalin, Heterologous expression of the Enterococcal vanA operon in methicillin-resistant Staphylococcus aureus, Antimicrob. Agents Chemother. 48 (2004) 4281-4285.
5. K. Hiramatsu, N. Aritaka, H. Hanaki, S. Kawasaki, Y. Hosoda, S. Hori, Y. Fukuchi, I. Kobayashi, Dissemination in Japanese hospitals of strains of Staphylococcus aureus heterogeneously resistant to vancomycin, Lancet 350 (1997) 1670–1673.
6. K. Sieradzki, R.B. Roberts, S.W. Haber, A. Tomasz, The development of vancomycin resistance in a patient with methicillin-resistant Staphylococcus aureus infection, N. Engl. J. Med. 340 (1999) 517-523.
7. K. Matsuzaki, Control of cell selectivity of antimicrobial peptides, Biochimica et Biophysica Acta, 1788 (2009) 1687-1692.
8. H. Jenssen, P. Hamill, R.E.W. Hancock, Peptide antimicrobial agents, Clin. Microbiol. Rev. 19 (2006) 491-511.
9. R.E.W. Hancock, H.-G. Sahl, Antimicrobial and host-defense peptides as new antiinfective therapeutic strategies, Nat. Biotechnol. 24 (2006) 1551–1557.
10. G.G. Perron, M. Zasloff, G. Bell, Experimental evolution of resistance to an antimicrobial peptide, Proc. Biol. Sci. 273 (2006) 251–256.
11. A.A. Bahar, D. Ren, Antimicrobial peptides, Pharmaceuticals 6 (2013) 1543-1575.

12. S. Rotem, A. Mor, Antimicrobial peptide mimics for improved therapeutic properties. Biochim. Biophys. Acta. 1788 (2009) 1582-1592.
13. W. van't Hof, E.C. Veerman, E.J. Helmerhorst, A.V. Amerongen, Antimicrobial peptides: Properties and applicability, Biol. Chem. 382 (2001) 597-619.
14. A.C. Engler, J.P.K. Tan, Z. Y. Ong, D.J. Coady, V.W.L. Ng, Y-Y Yang, J.L. Hedrick, Antimicrobial polycarbonates: Investigating the impact of balancing charge and hydrophobicity using a same-centered polymer approach, Biomacromolecules, 14 (2013) 4331-4339.
15. D. Druvari, N.D. Koromilas, G. Ch. Lainioti, G. Bokias, G. Vasilopoulos, A. Vantarakis, I. Baras, N. Dourala, J.K. Kallitsis. Polymeric quaternary ammonium-containing coatings with potential dual contact-based and release-based antimicrobial activity, ACS Appl. Mater. Interfaces, 8 (2016) 35593–35605.
16. N.C. Süer, C. Demir, N.A. Ünübol, Ö. Yalçın, T. Kocagöz, T. Eren, Antimicrobial activities of phosphonium containing polynorbornenes, RSC Advances, 6 (2016) 86151-86157.
17. J. Haldar, D. An, L.Á. de Cienfuegos, J. Chen, A.M. Klibanov, Polymeric coatings that inactivate both influenza virus and pathogenic bacteria. Proc. Natl. Acad. Sci., 103 (2006) 17667-17671.
18. B.C. Allison, B.M. Applegate, J.P. Youngblood, Hemocompatibility of hydrophilic antimicrobial copolymers of alkylated 4-vinylpyridine. Biomacromolecules 8 (2007) 2995-2999.
19. A. Sharma, G.R. Wilson, A. Dubey, Antibacterial activity of vinyl imidazole(VI) functionalized silica polymer nanocomposites (SBA/VI) against Gram negative and Gram positive bacteria, New J. Chem. 40 (2016) 764-769.
20. L. Liu, H. Wu, S.N. Riduan, J.Y. Ying, Y. Zhang, Short imidazolium chains effectively clear fungal biofilm in keratitis treatment, Biomaterials 34 (2013) 1018-1023.
21. L. Liu, Y. Huang, S.N. Riduan, S. Gao, Y. Yang, W. Fan, Y. Zhang, Main-chain imidazolium oligomer material as a selective biomimetic antimicrobial agent, Biomaterials 33 (2012) 8625-8631.
22. M. S. Ganewatta, C. B. Tang, Controlling macromolecular structures towards effective antimicrobial polymers, Polymer 63 (2015) A1-A29.
23. El-R. Kenawy, F. I. Abdel-Hay, A. El-R. R. El-Shanshoury, M. H. El-Newehya, Biologically active polymers: Synthesis and antimicrobial activity of modified glycidyl

methacrylate polymers having a quaternary ammonium and phosphonium groups, J. Control. Release 50 (1998) 145-152.

24. Y. Xue, H. Xiao, Y. Zhang, Antimicrobial polymeric materials with quaternary ammonium and phosphonium salts, Int. J. Mol. Sci. 16 (2015) 3626-3655.
25. A. Jain, L.S. Duvvuri, S. Farah, N. Beyth, A.J. Domb, W. Khan, Antimicrobial polymers. Adv. Healthc. Mater. 3 (2014) 1969–1985.
26. El-R. Kenawya, S. Kandil, Synthesis, antimicrobial activity and applications of polymers with ammonium and phosphonium groups, In: A. Muñoz-Bonilla, M.L. Cerrada, M. Fernández-García (Eds.), Polymeric Materials with Antimicrobial Activity: From Synthesis to Applications, RSC Publishing, Cambridge, 2013, pp. 54-74.
27. S.N. Riduan, Y. Yuan, F. Zhou, J. Leong, H. Su, Y. Zhang, Ultrafast killing and self-gelling antimicrobial imidazolium oligomers, Small 12 (2016) 1928-1934.
28. Y. Yuan, Y. Zhang, Synthesis of imidazolium oligomers with planar and stereo cores and their antimicrobial applications, ChemMedChem 12 (2017) 835-840.
29. J. McNulty, D. McLeod, A scalable process for the synthesis of (E)-pterostilbene involving aqueous Wittig olefination chemistry, Tetrahedron Lett. (2013) 6303-6306.
30. A.M. Deberardinis, M. Turlington, J. Ko, L. Sole, L Pu, facile synthesis of a family of h8binol-amine compounds and catalytic asymmetric arylzinc addition to aldehydes, J. Org. Chem. 75 (2010) 2836-2850.
31. K. Fukushima, S. Liu, H. Wu, A. C. Engler, D. J. Coady, H. Maune, J. Pitera, A. Nelson, N. Wiradharma, S. Venkataraman, Y. Huang, W. Fan, J. Y. Ying, Y. Y. Yang, J. L. Hedrick, Nature Comm. 4 (2013) 2861.
32. J.S. Cho, J. Zussman, N.P. Donegan, R.I. Ramos, N.C. Garcia, D.Z. Uslan, Y. Iwakura, S.I. Simon, A.L. Cheung, R.L. Modlin, J. Kim, L.S. Miller, Noninvasive in vivo imaging to evaluate immune responses and antimicrobial therapy against Staphylococcus aureus and USA300 MRSA skin infections, J. Invest Dermatol. 131 (2011) 907-915.
33. L.M. Barker, O.Z. Nanassy, M.W. Reed, S.J. Geelhood, R.D. Pfalzgraf, G.A. Cangelosi, D. De Korte. Multiple pH measurement during storage may detect bacterially contaminated platelet concentrates, Transfusion 50 (2010) 2731-2737.

## Graphical Abstract